運輸省港湾技術研究所　(25th Anniversary Issue)

港湾技術研究所報告

REPORT OF THE PORT AND HARBOUR RESEARCH INSTITUTE

MINISTRY OF TRANSPORT

VOL. 26　NO. 5　DEC. 1987

NAGASE, YOKOSUKA, JAPAN

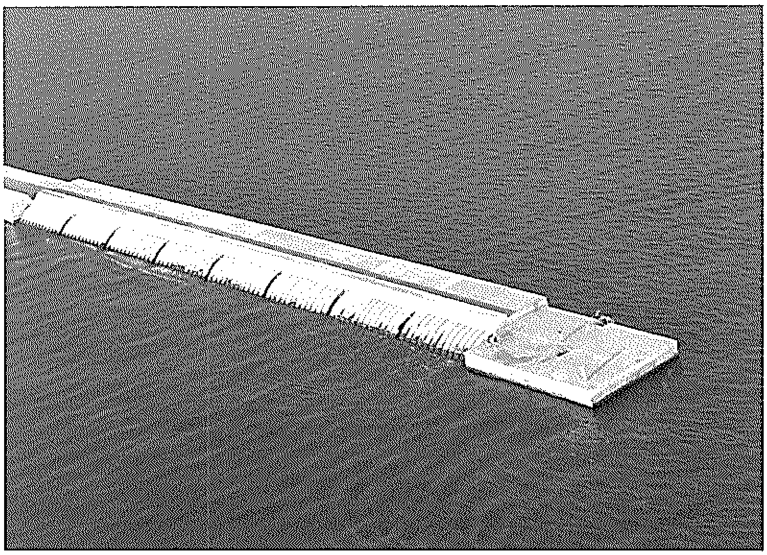

Curved Slit Caisson Breakwater

View of curved slit caisson breakwater completed in the construction at the port of Funakawa. (Courtesy of Akita Port Construction Office, the First District Port Construction Bureau, Ministry of Transport)

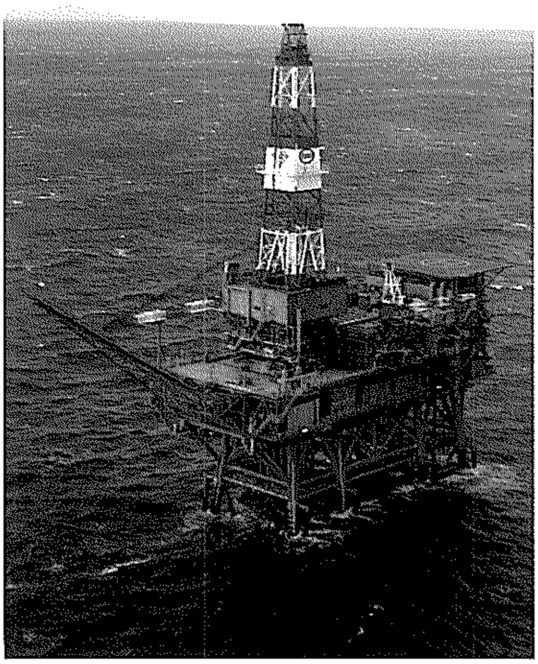

Facilities for Ocean Directional Wave Measurement

Four step type wave gauges and a two-axis directional current meter with a pressure sensor are installed on the legs of an offshore oil rig. They are operated simultaneously for detailed directional wave analysis.

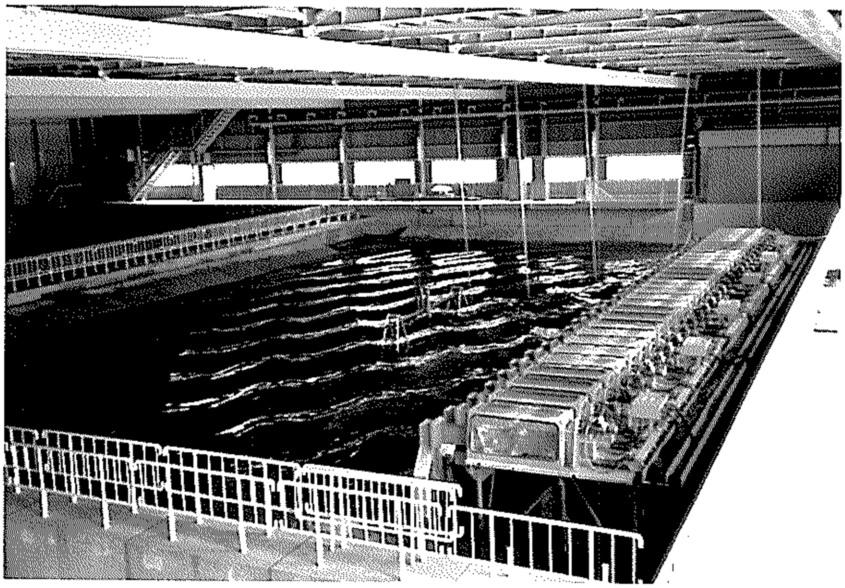

Serpent-type Wave Generator

The photograph shows the serpent-type wave generator in the short-crested wave basin and the superimposition state of two different oblique waves generated by the generator.

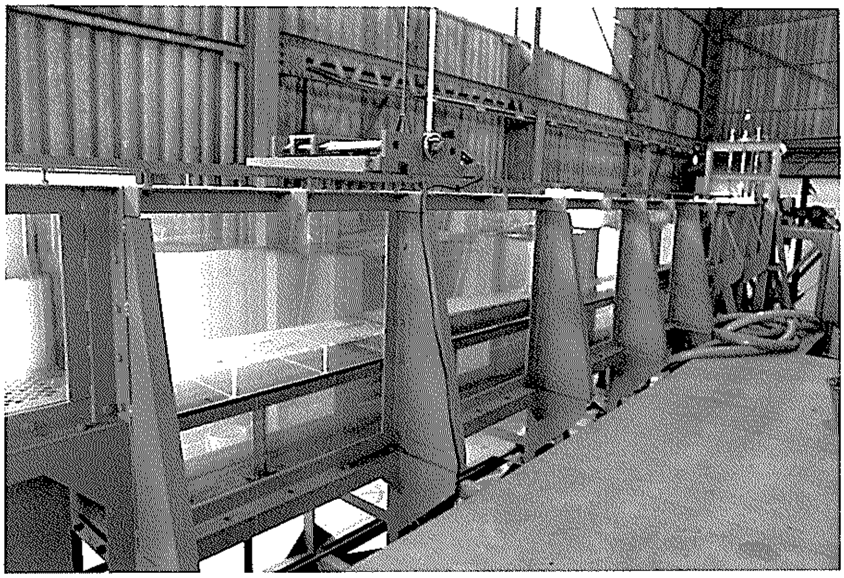

Wave-soil Tank

The experiments concerning the wave-soil interactions are conducted in this tank. The soil tank and the test section are located at the center of the tank. A movable floor is provided at the bottom of the test section and the level of the interface of mud layer and water can easily be adjusted to the level of the flume bottom.

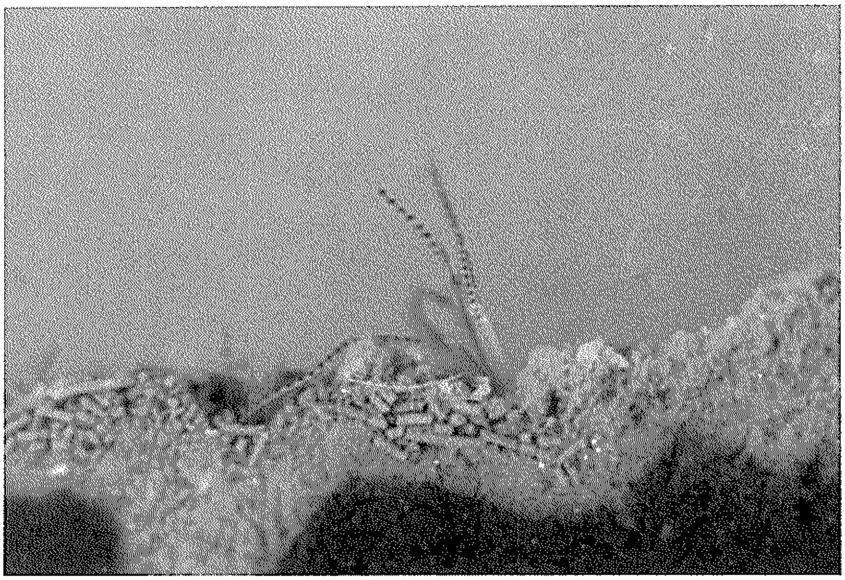

Pararionospio Pinnata

The biomass of benthos is one of the most sensitive indices to know the effect of sea-bed sediment treatments on the marine environmental improvement. The picure shows a kind of benthos, *pararionospio pinnata,* which preferentially exists in the polluted sea-bed.

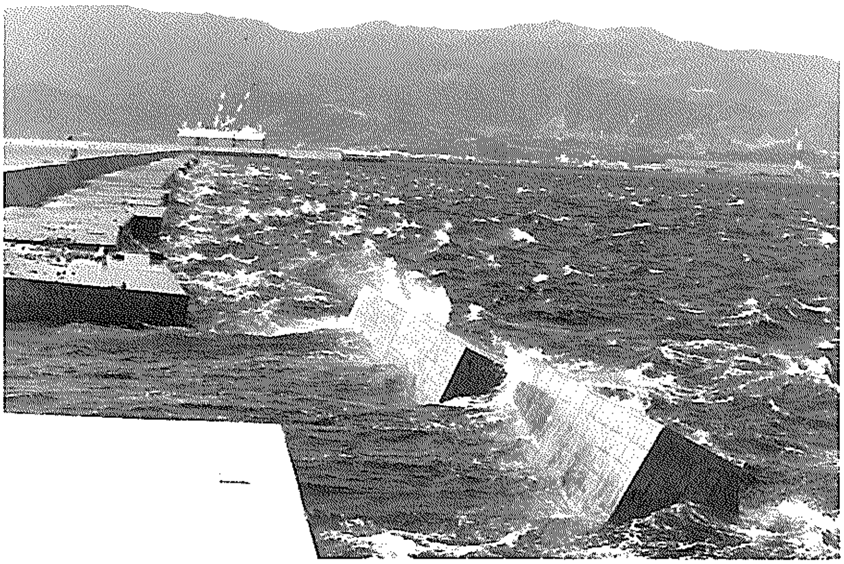

Breakwater Damaged by Storm

This photograph shows a breakwater damage by a storm.
The breakwater is of the composite type with concrete caisson on a rubble mound. Two caissons were severly damaged due to the instability of a rubble mound.

Nondestructive Evaluation of Pavement

Nondestructive methods for evaluating the load carrying capacity of airport concrete pavements have been developed by using Falling Weight Deflectometer(FWD).

Seismic Damage to Gravity Quaywall

The 1983 Nipponkai-Chubu earthquake(Magnitude : 7.7)caused serious damage to port facilities in northern part of Japan. This photo shows the damage to gravity quaywall. The concrete cellular block walls were collapsed and completely submerged.

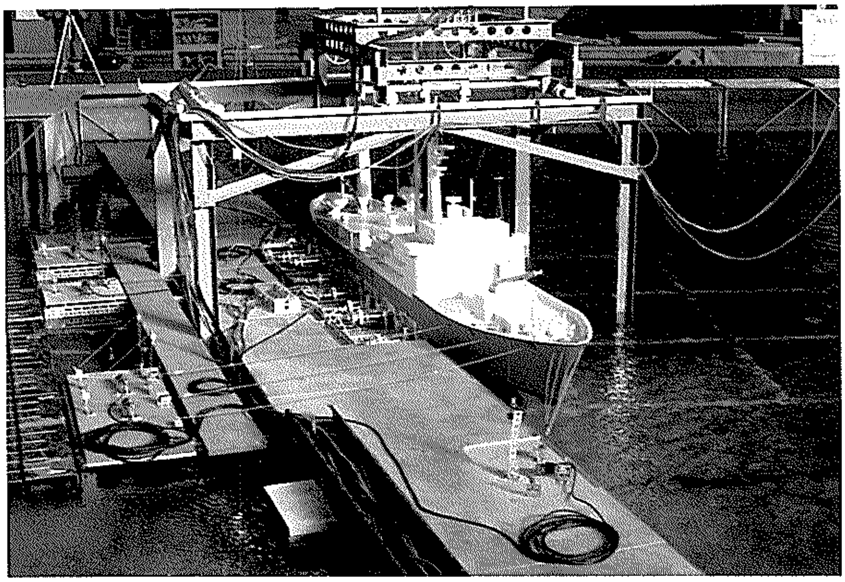

Model Experiment of Mooring Ship

Model ship is moored at a quay wall with fenders and mooring ropes subjected to gusty wind and/or irregular waves.

Vessel Congestion in Japan

As Japan is surrounded by the sea, there are many crowded water areas with various sizes and types of vessels. Arround there, many construction works were planned such as ports and harbours, off-shore airports, huge bridges and so on, so that many marine traffic observations and marine traffic simulations have been carried out.

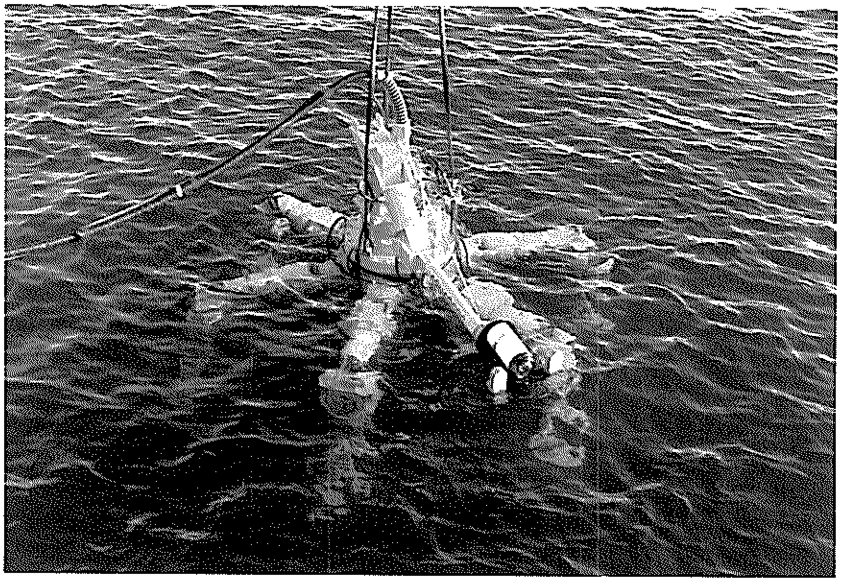

Underwater Inspection Robot

This is the six-legged articulated underwater inspection robot named "AQUAROBOT". The robot controlled by a computer can walk on uneven sea bed without making water muddy.

Foreword

The Port and Harbour Research Institute is a national laboratory under the Ministry of Transport, Japan. It is responsible for solving various engineering problems related to port and harbour projects so that governmental agencies in charge of port development can execute the projects smoothly and rationally. Its research activities also cover the studies on civil engineering facilities of air ports.

Last April we have celebrated the 25th anniversary of our institute because the present organization was established in 1962, though systematic research works on ports and harbours under the Ministry of Transport began in 1946. As an event for the celebration, we decided to publish a special edition of the Report of the Port and Harbour Research Institute, which contains full English papers only. These papers are so selected to introduce the versatility of our activities and engineering practices in Japan to overseas engineers and scientists. It is also intended to remedy to a certain extent the information gap between overseas colleagues and us.

The reader will find that our research fields cover physical oceanography, coastal and ocean engineering, geotechnical engineering, earthquake engineering, materials engineering, dredging technology and mechanical engineering, planning and systems analysis, and structural analysis. Such an expansion of the scope of research fields has been inevitable, because we are trying to cover every aspect of technical problems of ports and harbours as an integrated body.

The present volume contains eleven papers representing six research divisions of the institute. The materials introduced in these papers are not necessarily original in strict sense, as some parts have been published in Japanese in the Reports or the Technical Notes of the Port and Harbour Research Institute. Nevertheless they are all original papers in English and are given the full format accordingly. We expect that they will be referred to as usual where they deserve so.

It is my sincere wish that this special edition of the Report of the Port and Harbour Research Institute will bring overseas engineers and scientists more acquainted with our research activities and enhance the mutual cooperation for technology development related to ports and harbours.

December 1987
Yoshimi Goda
Director General

港湾技術研究所報告 (REPORT OF P. H. R. I.)

第26巻　第5号 (Vol. 26, No. 5) 1987年12月 (Dce. 1987)

目　次 (CONTENTS)

REPORT OF THE PORT AND
HARBOUR RESEARCH INSTITUTE
Vol. 26, No. 5 (Dec. 1987)

8. Study on Rational Earthquake Resistant Design Based on the Quantitative Assessment of Potential Seismic Damage to Gravity Quaywalls

Tatsuo UWABE*

Synopsis

Procedures for the quantitative estimation of the earthquake damage to gravity quaywalls were studied as a preparation against earthquakes. Cases of earthquake damage to gravity quaywalls were collectd for past earthquakes, and the quantity, to give the level of the earthquake damage, and the classification of the failure mode were then analysed. An estimation method to give the quantity of the damage (displacement and cost) was presented, using the ratio of the corresponding seismic coefficient of the ground acceleration to the seismic coefficient which gives the safety factor of one in the stability analysis of the design standard. An optimum seismic coefficient from an economic viewpoint was then studied for the rational seismic design, on the basis of the quantitative estimation method of the cost of damage.

* Chief of Earthquake Disaster Prevention Laboratory, Structures Division

港湾技術研究所報告
第26巻 第5号 (1987.12)

8. 重力式係船岸の地震被災量の推定手法に関する研究

上 部 達 生*

要 旨

地震防災対策をより合理的かつ効果的に実施すること，およびより合理的な耐震設計法を開発することを目的として，重力式係船岸の地震時の被災量の定量的な推定手法について検討した。まず，地震被災事例を収集し，その被災の定量的表現，被災形態の類別を行った。被災を定量的に取り扱うために，被災変形量（最大はらみ出し量，天端沈下量，エプロン沈下量等）および被災額をとりあげた。被災形態に関する検討では，重力式係船岸の地震時の被災は滑動が主因とみられる事例が，支持力不足が主因とみられる事例より多いことが明らかになった。

収集した地震被災事例に基づいて，地震動の強さに相当する震度（作用震度）とその構造物の安定解析において安全率が1となる時の震度（破壊震度）との比から重力式係船岸の被災変形量および被災額を推定する手法について検討した。

さらに，地震被災事例に基づく検討で得られた被災量推定手法を，より合理的な耐震設計に利用することを目的として，経済的観点からの最適設計震度について検討した。地震被災事例に基づいた推定手法から得られる被災額と，最大加速度の発生確率から，被災額の期待値を計算し，これと初期建設費の和が最小となる設計震度を最適値として求める手法と，その具体的な計算例を示した。

*構造部 地震防災研究室長

Contents

1. Introduction

Currently in Japan, there is a high possibility of the occurrence of a large earthquake in Tokai Area, a central part of Japan, in the near future, and thus many kinds of investigations for earthquake preparedness have been done. One of the investigations related to ports that may become key locations for the transportation of emergency goods immediately after an earthquake, is a survey on the earthquake resistance capability of port facilities to estimate the number of port facilities available after the earthquake. In this survey, the seismic stability of port facilities has been judged by the evaluation method reported by Tsuchida et al.[1] According to this method there are only the two kinds of analyzed results of no damage, and collapse. However the actual seismic damage of port facilities shows a gradual change from no damage to collapse.

It is now necessary to assess the potential seismic damage quantitatively by the following reasons.

i) If the extent of damage to port facilities is small, they can still serve for the temporary transportation of urgent goods. It is therefore important to know whether the port facilities are available after earthquakes, by prior estimation of the extent of damage.

ii) Because the number of port facilities which are assessed to be damaged is large and because they cannot be reinforced at the same time, it is necessary to decide the priority of reinforcement and an effective reinforcing method according to the extent of potential damage.

With the background described above, the present study is concerned with the development of a quantitative estimation method of seismic damage to port facilities. It is further aimed at establishing the rational earthquake resistant design by utilizing the quantitative estimation method of seismic damage thus developed. In the present study, an optimum seismic coefficient from an economical viewpoint is sought for, using the quantitatively estimated potential seismic damage. The structure analyzed in this study is a gravity type quaywall, which is a typical berthing facility in Japan.

In this report, historical cases of seismic damage to gravity quaywalls and technical lessons derived from such damages are first described, and the failure mode is then discussed. Based on these data of seismic damage to gravity quaywalls, a quantitative estimation method of seismic damage to gravity quaywalls is then presented. Lastly, an optimum seismic coefficient is derived by applying the quantitative estimation method to several cases of gravity structures with the cost analyses.

2. Cases of seismic damage to gravity quaywalls, and technical lessons from such damage

2.1 Earthquake, ports and gravity quaywalls discussed in this report

A gravity quaywall is a typical berthing facility to moor ships in Japan. The structural types of gravity quaywalls are classified into the caisson type, the concrete block type, the L-shaped concrete block type, the cellular block type and the wave absorbing vertical wall type. Figure 1 illustrates the caisson type of gravity

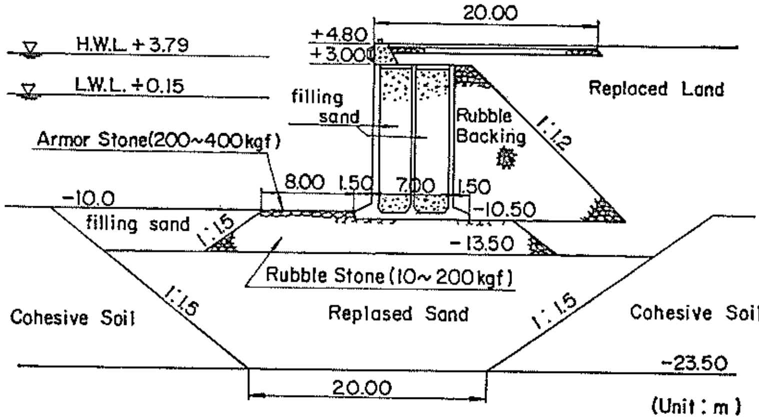

Fig. 1 Example of gravity quaywall (Caisson type)

Table 1 Data of seismic damage to port facilities

Number of earthquakes	Number of ports	Structural types	Number of damage data
17	100	Quaywall	
		Gravity type	275(77)
		Steel sheet pile type	161(56)
		Cellular type	11(7)
		Piled pire type	31(17)
		Breakwater	40(11)
		Other types	161(39)
		Total	679(207)

Figures within parentheses are no damage data and are included in total of each type.

quaywalls.

Table 1 shows the number of port facilities damaged by past earthquakes. The figure inside the parentheses in Table 1 shows the number of no damage facilities and is within the total number. The details of these 679 data were shown in the report of Uwabe[2]. The number of gravity quaywalls discussed here was 275 and this number includes 77 with no damage data. In the study for the quantitative estimation of seismic damage to gravity quaywalls the episodes of gravity quaywalls clearly damaged by liquefaction were excluded from this report.

2.2 Seismic damage episodes, and technical lessons from such damage

Figure 2 shows the damage to concrete block type quaywalls. The damage level were comparatively large, but there was no collapse. The same type of quaywall adjacent to that in Fig. 2 were constructed directly on the rock, and collapsed completely. It was believed that this difference in the damage to the two quaywalls was due to the buffer effect of the rubble stone mound under the concrete blocks. Figure 3

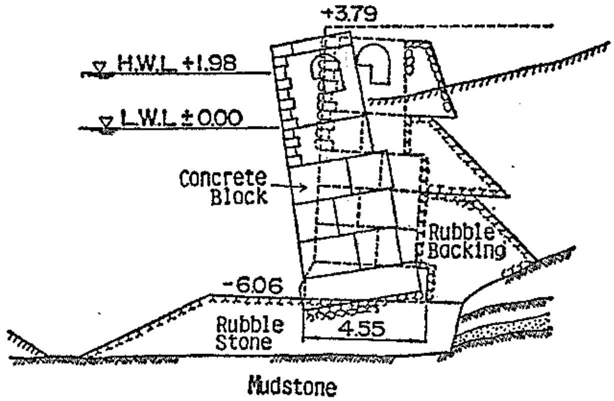

Fig. 2 Damage of gravity quaywall (Concrete block type)

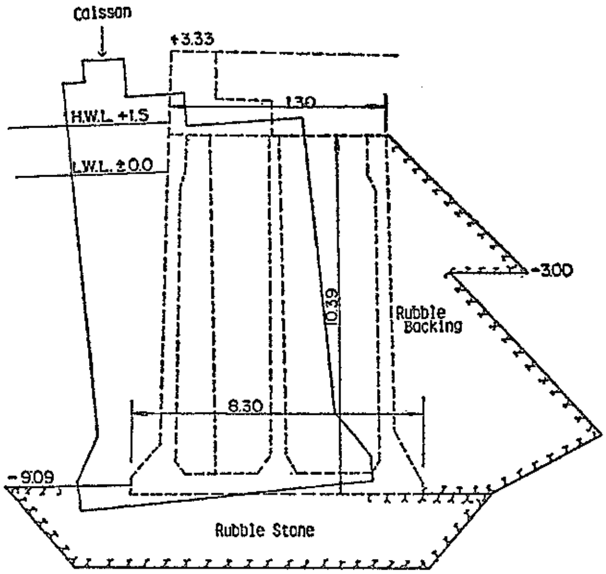

Fig. 3 Damage of gravity quaywall (Caisson type)

shows a typical example of a caisson type gravity quaywall damaged by a past earthquake. Figure 4 shows the damage of the gravity quaywall with a pile foundation. Sliding of the wall developed, but no settlement of the wall was observed. No settlement of this quaywall was due to the pile foundation.

Though the cases of damage affected by liquefaction were excluded from this report, this paragraph shows the outline of the liquefaction damage to quaywalls. Figure 5 shows the liquefaction damage of the concrete block type quaywall. The dotted lines denote the original design configuration and solid lines shows the profile after the damage. The wall submerged and tilted. The liquefaction therefore

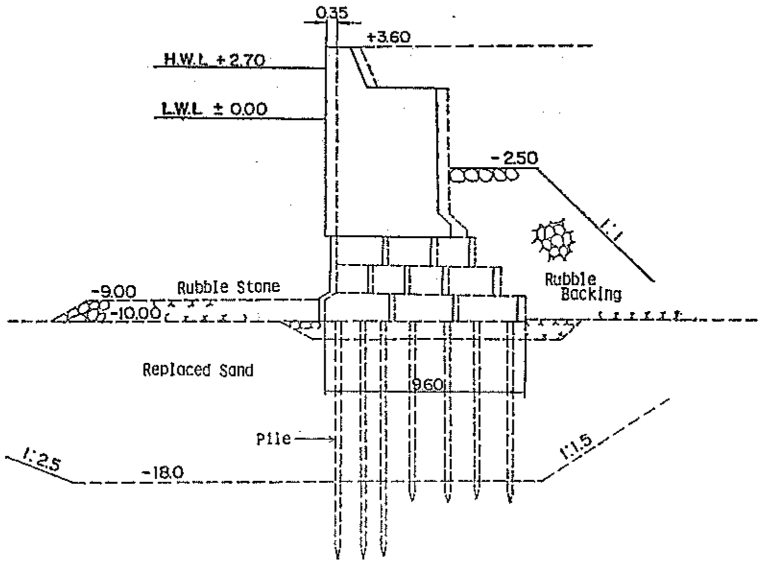

Fig. 4 Damage of gravity quaywall (Pile foundation)

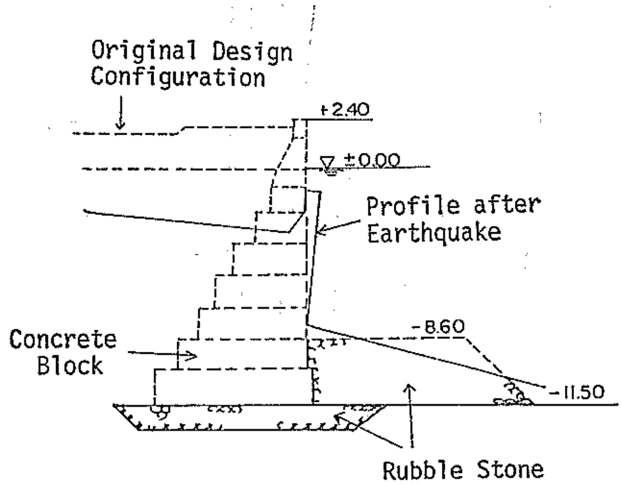

Fig. 5 Gravity quaywall damaged by liquefaction

severely affects the seismic stability of port facilites and so a study for the liquefaction for the port facilities is very important. The last study for the liquefaction of port facilities was a new criteria for assessing the liquefaction potential, and was reported by Iai, Koizumi and Tsuchida[3].

It is very important to know the input earthquake motion for the seismic design. From this point of view, strong-motion earthquakes have been observed in major ports in Japan, and about 3000 accelerograms were accumulated. A report on strong-motion earthquake records in Japanese ports has been published annually[4].

2.3 Quantification of damage to gravity quaywalls

(1) Damage extent

When seismic damage to the port facilities in Niigata earthquake was reported[5),6)] the extent of the damage to port facilities (termed damage extent) was classified into five categories between no damage and complete collapse. Table 2 shows the criteria to classify the damage extent. These criteria are based on the degree of "displacement and deformation relative to the original configulation".

Table 3 shows the classified results of the damage extent for each structural type of gravity quaywalls accumulated in this report. According to Table 3, no damage data and the data whose damage extent is "I" amount to about one third of the total damage of data respectively, while the damage episodes whose damage extent is "III" and "IV" are few.

(2) Seismic damage deformation

In a survey of seismic damage the swelling and settlement of face line of the wharf, the tilting of wall, the settlement of apron and other factors were measured as shown in Fig. 6, and the length of damaged section in one berth (damage length) was also measured.

In this report, the parameters which can be used to quantify the damage

Table 2 Classification of damage

Damage Extent	Description of Damage
0	No damage
I	Damage and changes are limited to appurtenances, the main part of the structure remaining intact.
II	"Considerable" change has occurred to the main part of the structure.
III	The main part of the structure is deemed to have been destroyed, although the original outline has been retained.
IV	Destruction is total, leaving no semblance of the original configuration.

Table 3 Structural type and damage extent

Structural type / Damage extent	Caisson	Concrete block	L-shaped concrete block	Prepacked concrete	Others	Total
0	22	31	11	11	2	77
I	24	42	9	7	11	93
II	15	16	3	3	5	42
III	3	13	5	1	8	30
IV	5	11	1	2	2	21
Unknown	0	6	0	1	5	12
Total	69	119	29	25	33	275

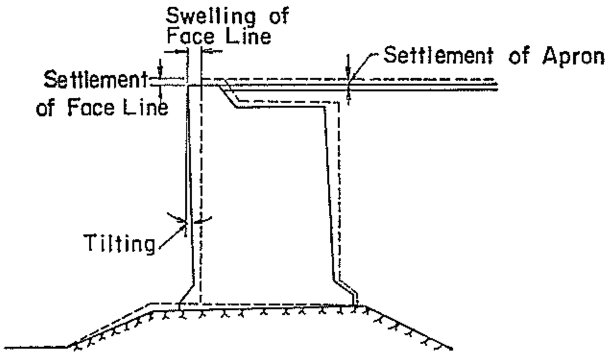

Fig. 6 Seismic damage deformation of gravity quaywall

deformation were defined as follows:

i) Maximum swelling (the maximum value of the swelling of face line in the damage length)

ii) Average swelling (the averaged value of the swelling of face ine in the damage length)

iii) Settlement of the face line (the maximum value of the settlement at the face line of gravity quaywall in the damage length)

iv) Settlement of apron (the maximum value of the settlement at the apron in the damage length)

v) Tilting (the maximum value of the tilt angle of wall in the damage length)

The following were also discussed.

vi) Damage length of quaywall

vii) Damage deformation ratio (the ratio of the maximum swelling to the wall height which is the height between the sea bottom and the wall head)

viii) Sum of deformation (the sum of the maximum swelling, the settlement of face line and the settlement of apron)

(3) Cost of seismic damage to gravity quaywalls

The cost of seismic damage to gravity quaywalls (seismic cost) means the outlay assessed officially as repair work by the government. In this report, the seismic cost was defined as the sum of the repair work cost divided by the damage length of gravity quaywall (unit: thousand yen/m). In this study, the ratio of the seismic cost to the initial construction cost was also discussed. This ratio is termed the cost rate of seismic damage (seismic cost rate).

The costs shown in the earthquake damage reports are the sums of the day. It was therefore required to convert these costs to same price level. Then, the fluctuation of the past years was investigated in the construction prices, in the wholesale prices of construction materials and in the wages respectively, and the fluctuation was quantified by a price index that is 100 for the prices at the year 1980. The repair cost and the initial construction cost were converted to same price level by this price index.

3. Seismic failure mode of gravity quaywalls

3.1 Classification of seismic failure mode

The principal failure modes of gravity quaywalls during earthquakes are:

i) Sliding of wall
ii) Settlement and tilting of wall by insufficient bearing capacity of foundation
iii) Overturning of wall

In this report these failure modes were studied on the basis of the report of Mitsuhashi and Nakayama[7]. The classification presented by Mitsuhashi et al. is shown in Fig. 7. The overturning of the wall shown in Fig. 7 was not included in the original classification of Mitsuhashi et al.

3.2 Classified result of seismic failure mode

Figure 8 illustrates the classification flow diagram to determine the seismic failure modes. X, Y and P in Fig. 8 are given based on Fig. 9 as follows:

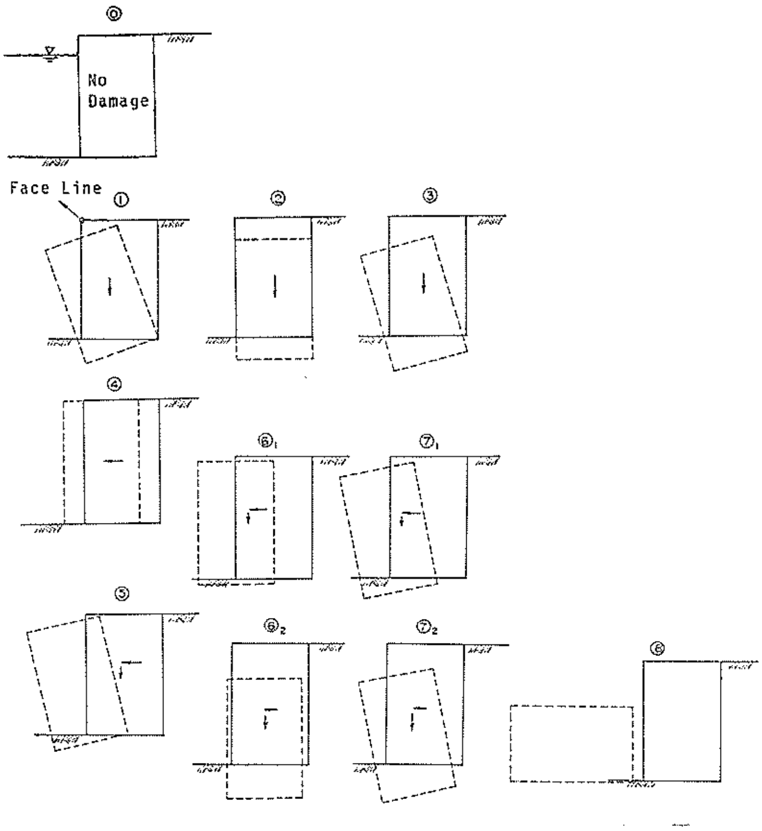

Fig. 7 Failure mode of gravity

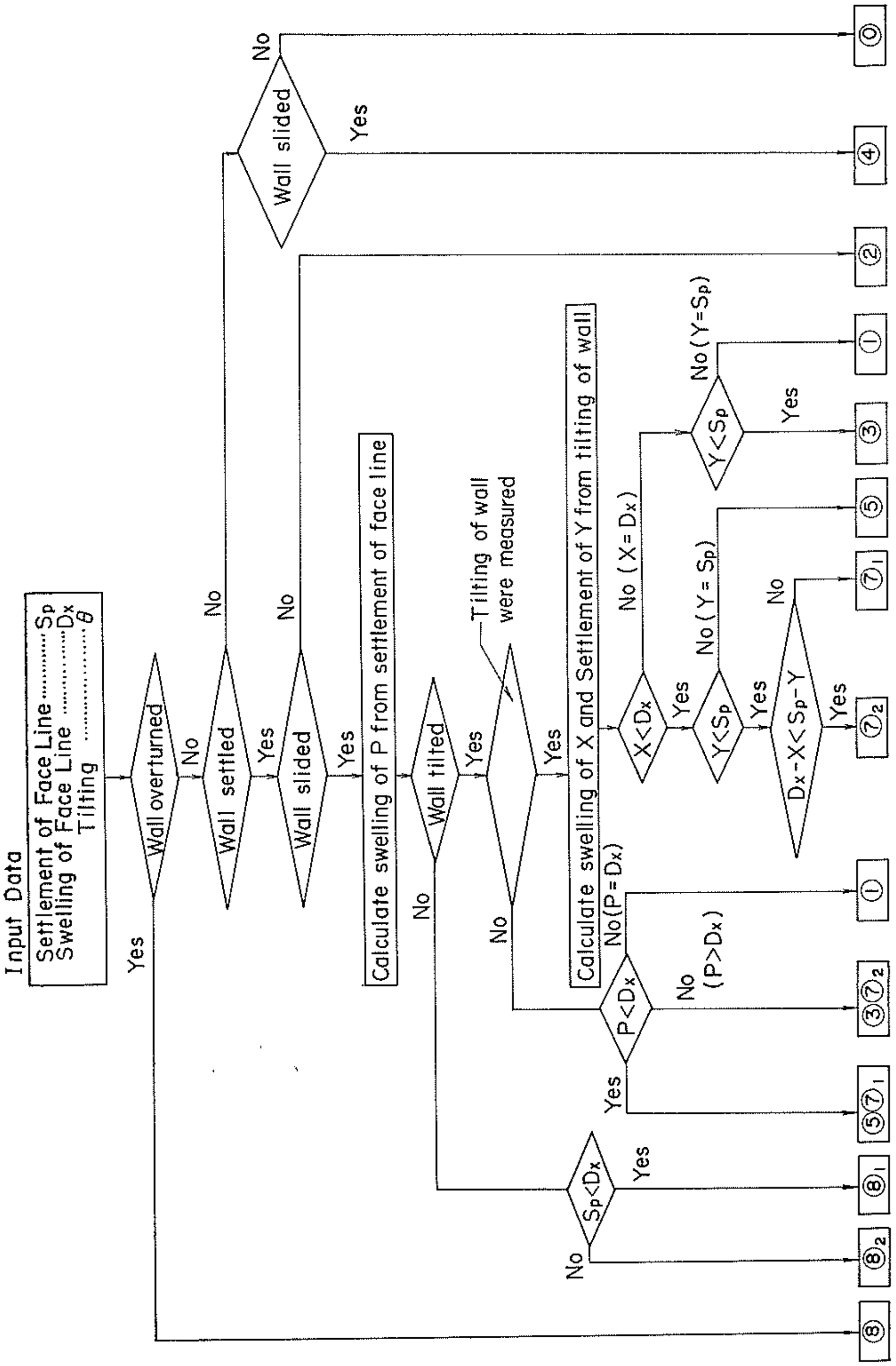

Fig. 8 Classification flow diagram of failure mode

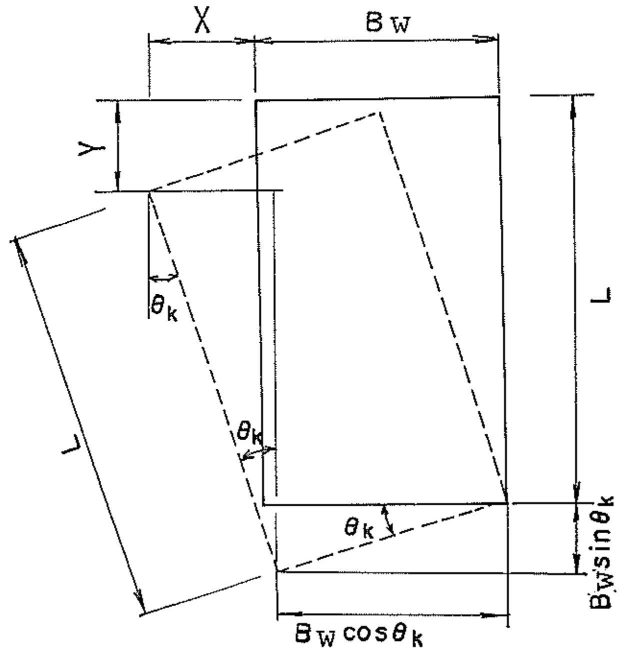

Fig. 9 *X*, *Y*, and *P* in **Fig. 8**

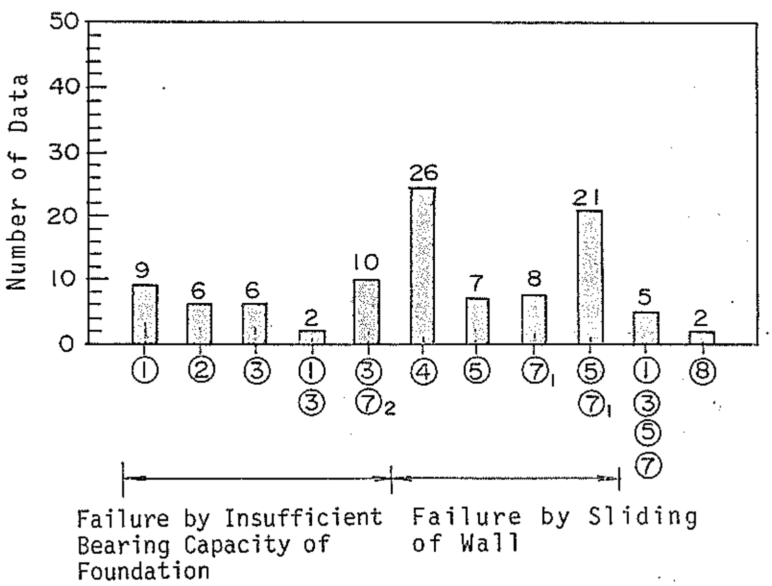

Fig. 10 Classification result of failure mode

$$X = L \sin \theta_k + B_w \cos \theta_k - B_w \qquad (1)$$
$$Y = B_w \sin \theta_k + L - L \cos \theta_k \qquad (2)$$
$$P = \frac{L}{B_w} \cdot S_p \qquad (3)$$

where, X: Swelling of face line
Y: Settlement of face line
θ_k: Tilt angle of wall
L: Wall height
B_w: Wall width
P: Swelling in case that tilt angle is small
S_p: Measured settlement

Figure 10 shows the result to classify the cases of damage to gravity quaywall according to the flow diagram in Fig. 8. According to Fig. 10 the number of classified data as ④, ⑤, ⑦$_1$ and ⑤ ⑦$_1$ where the principal cause of the damage was the sliding of the wall was 62 (61% of total) and the number of data classified as ①, ②, ③, ① ③, ③ ⑦$_2$ where the principal cause was the insufficient bearing capacity of foundation was 33 (32% of total). It was therefore concluded that the greater numbers of damage to gravity quaywalls were associated with the sliding of the wall, than with foundation failure.

4. Quantitative estimation of seismic damage to gravity quaywall by analysis of past damage data

4.1 Assessment of damage occurrence

Figure 11 shows the flow diagram of the procedures used in assessing the potential damage to given port facilities for earthquake preparedness. The portion above the broken line relates to the procedure leading to the judgement as to whether or not damage has occurred and describes here; the portion below the broken line to quantification of the damage which has occurred and is described in next paragraph.

The judgement on the occurrence of damage generally follows two steps. One, as shown on the right column in Fig. 11, aims to determine the working seismic coefficient at the site of interest under a given earthquake. The other aims to the breaking seismic coefficient for a given structure, i.e. the seismic coefficient corresponding to the structure safety factor of 1 in accordance with the current design criteria of port facilities in Japan.

A working seismic coefficient means the seismic coefficient which works on structures during earthquakes, and the relation between the working seismic coefficient and the maximum ground acceleration was presented as follows[8]:

$$\left.\begin{aligned} K_e &= \frac{\alpha}{g} && (a < 200\,\mathrm{Gal}) \\ K_e &= \frac{1}{3}\left(\frac{\alpha}{g}\right)^{1/3} && (a \geqq 200\,\mathrm{Gal}) \end{aligned}\right\} \qquad (4)$$

where, K_e: Working seismic coefficient

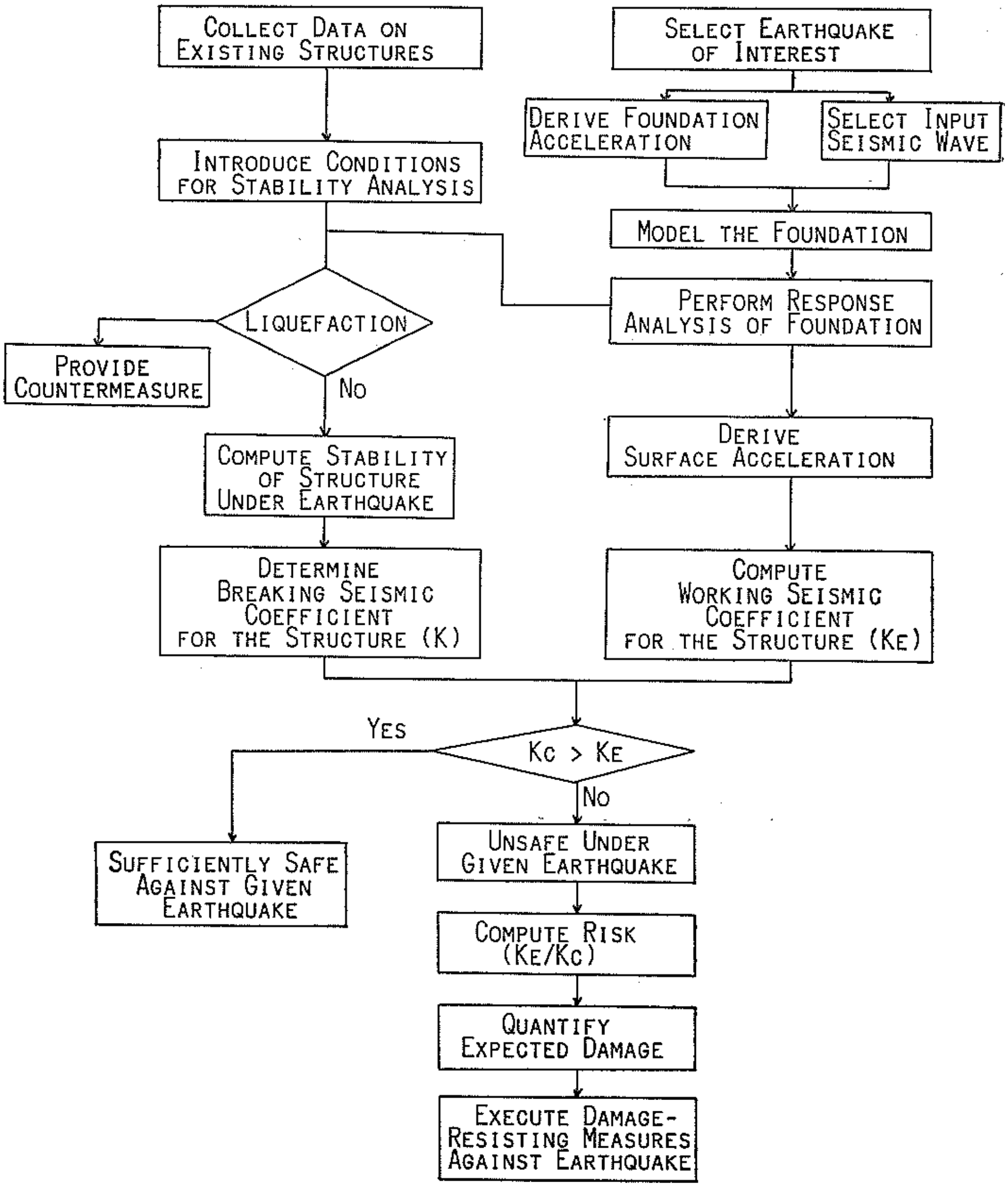

Fig. 11 Flow diagram for assessment of potential earthquake damage to port facilities

α : **Maximum ground acceleration (Gal)**
g : **Acceleration of gravity (980 Gal)**

These relationships have been derived from comparison between the on-site seismic coefficients determined from the stability analysis of damaged structures using the current design criteria for a safety factor of 1, while the ground acceleration is either estimated or measured.

For gravity quaywalls, the stability analysis should aim to derive the sliding and overturning behaviors as well as the bearing strength of the foundation, and also determine the seismic coefficient causing each of these failure under the safety factor of 1. This seismic coefficient is termed the critical seismic coefficient.

Critical seismic coefficients are given respectively in three stability examinations mentioned above. When the smallest of these critical seismic coefficients is smaller than the working seismic coefficient, the structure starts to break during earthquakes. This is defined as the breaking seismic coefficient.

The procedures in assessing the potential damage to a given structure is described as follows. First, the maximum ground acceleration at the site of interest is determined as a function of the earthquake magnitude, and the effective distance which is measured from the edge of the fault plane. Next, the input seismic wave is selected, and then an appropriate model for the foundation at the site is chosen. Response analysis is then performed to deduce the maximum ground surface acceleration, which is then input to obtain the working seismic coefficient.

The following procedure is used for the breaking seismic coefficient. First, collect the design data for the structure and establish conditions for the stability computation. Next, assess whether or not there would be liquefaction. If yes, assume that a countermeasure has been provided to prevent liquefaction before undertaking stability analysis under earthquake conditions. Then, determine the breaking seismic coefficient from the stability analysis using the current design criteria.

A decision on whether or not damage would occur is based on the comparison between the working seismic coefficient and the breaking seismic coefficient. If the breaking seismic coefficient is greater than the working seismic coefficient, the structure is considered safe and earthquake-resistant. Otherwise, the structure is expected to sustain damage due to the earthquake.

4.2 Quantitative estimation of seismic damage to gravity quaywall

As mentioned in Paragraph 4.1 the structure starts to breaking when the working seismic coefficient (K_e) is greater than the breaking seismic coefficient (K_c), and the quantitative damage that occurs to a structure is considered proportional to the ratio between K_e and K_c. Therefore, a method to estimate the damage extent was presented using this ratio between K_e and K_c, an index which is defined as the risk ratio (F_c). The relationship between the seismic damage deformation and the risk ratio was then investigated on the basis of the regression analysis of the historical seismic damage data. In this analysis, the maximum swelling, the average swelling, the settlement of the face line, the settlement of apron, the damage deformation ratio, the sum of deformation and the seismic cost rate were discussed.

Figures 12~14 show the relationship between quantities of seismic damage deformation and the risk ratio. These figures show the damage extent classified by the symbols. The data whose damage conditions were considered to be quite different from others by a detailed examination, shown with the circle in Figs. 12~14 were excluded on the regression analysis. Table 4 shows the equations represent regressions.

As shown in Table 4, correlation coefficients of the regression formula obtained here are not thoroughly high. In order to obtain a high accuracy, it is necessary

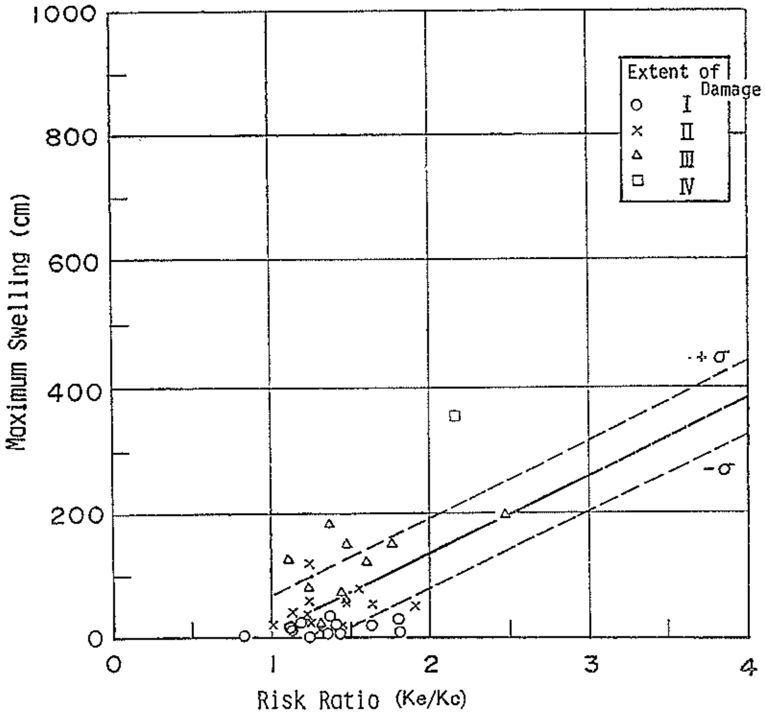

Fig. 12 Maximum swelling versus risk ratio

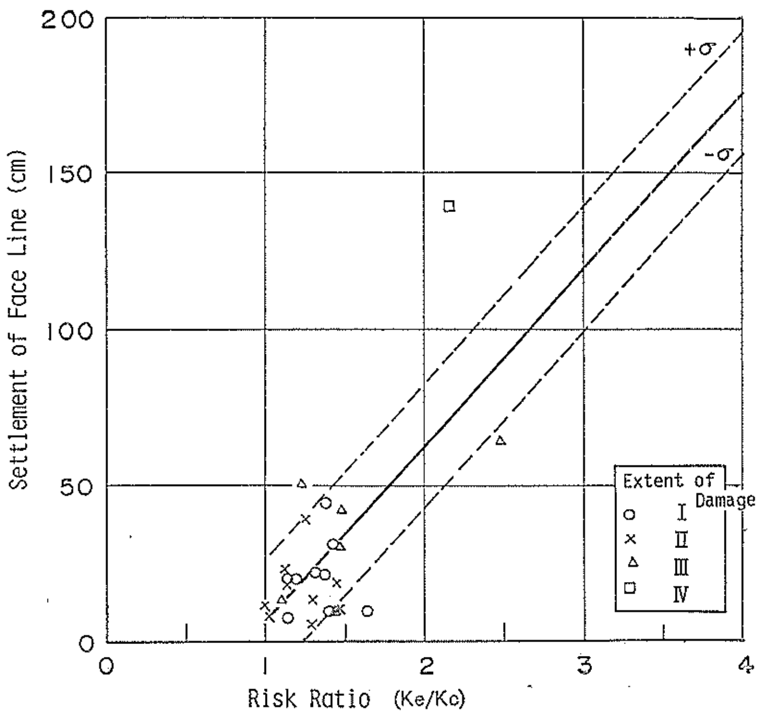

Fig. 13 Settlement of face line versus risk ratio

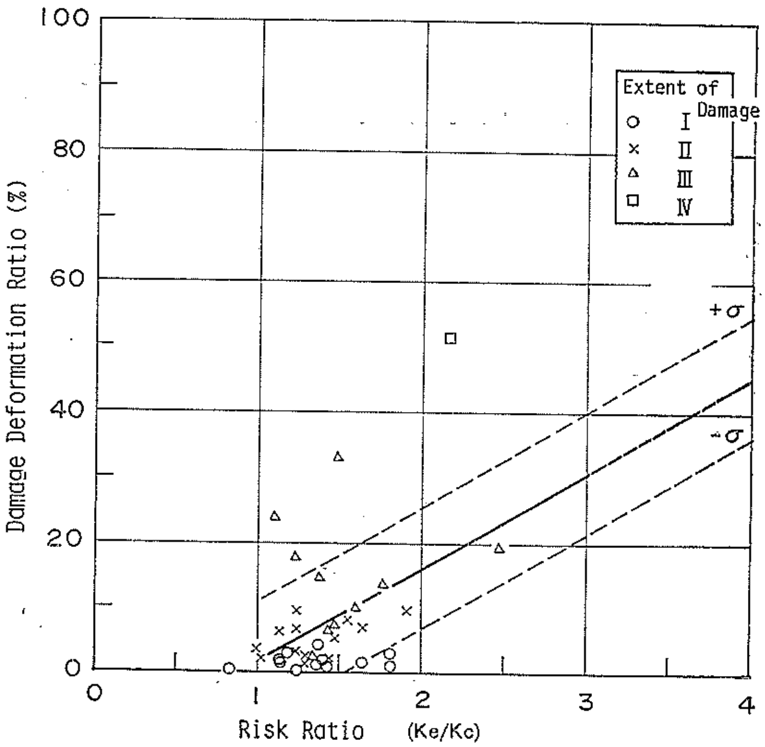

Fig. 14 Damage defomation ratio versus risk ratio

Table 4 Results of regression analysis

Criterion variables	Regression formula	Correlation coefficient	Standard deviation
Maximum swelling (D_x, cm)	$D_x=-113.8+124.4F_c$	0.559	59.1
Settlement of face line (S_p, cm)	$S_p=-50.9+57.1F_c$	0.677	20.0
Damage deformation ratio (R_g, %)	$R_g=-12.7+14.5F_c$	0.455	9.1
Sum of deformation (D_a, cm)	$D_a=-127.5+148.5F_c$	0.540	73.2

Predictor variables (F_c): Risk Ratio (K_e/K_c)

to reexpamine the relationship between the working seismic coefficient and the ground acceleration with high accuracy, to investigate the relationship between the seismic damage deformation and the risk ratio for each failure modes, considering other factors of the ground condition and so on. However, no one knows whether a large number of damage data for regressions with a higher accuracy will be obtained or not in the near future. Therefore, it may be proper in the present situation to use the regression formula obtained here.

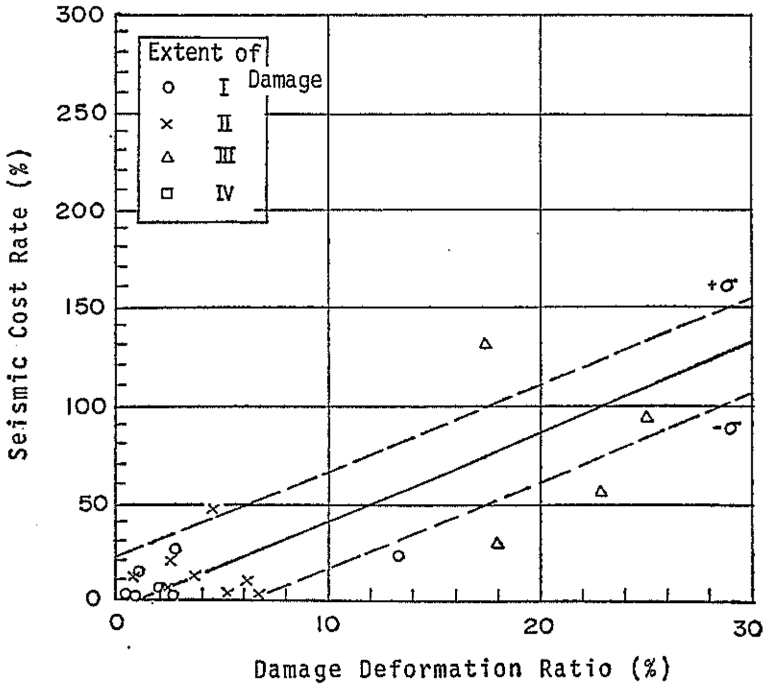

Fig. 15 Seismic cost rate versus damage deformation ratio

The regression formula that represents the relationship between the seismic cost rate (C_f) of the gravity quaywalls and the risk ratio (F_c) was not obtained with high accuracy because of insufficient number of data. Then, the relation between C_f and F_c was present from the two regression formulae that are the equations of C_f and the damage deformation ratio (R_g), and that of R_g and F_c.

Figure 15 shows the seismic cost rate against the damage deformation ratio. The solid straight line in Fig. 15 shows a regression formula whose correlation coefficient is 0.875. This formula is

$$C_f = -4.23 + 4.563 R_g \tag{5}$$

where, C_f: Seismic cost rate of gravity quaywalls
R_g: Damage deformation ratio

The regression formula of R_g and F_c ($=K_e/K_c$) in Table 4 is

$$R_g = -12.7 + 14.5 F_c \tag{6}$$

Accoridng to these two formulae, the relationship between C_f and F_c can be given as follows:

$$C_f = -62.2 + 66.2 F_c \tag{7}$$

It was believed that this formula was obtained by means of the best method in the present situation in order to estimate the cost of gravity quaywalls for a seismic coefficient that is optimum from the economical viewpoint discussed in Chapter 5.

5. Optimum seismic coefficient from economical viewpoint

The seismic coefficient of the design standard used for port facilities is determined as a product of a regional seismic coefficient, a ground classification factor and an important factor. This regional seismic coefficient was derived mainly from the expected value of the maximum seismic coefficients for the return period of 75 years reported by Kawasumi[9] (1951). As studies into earthquake engineering have progressed since Kawasumi's report so that many strong motion earthquake records have been obtained, more rational seismic coefficients are expected now. One of the seismic coefficients given by the rational method is the optimum seismic coefficient from the economical viewpoint. This optimum seismic coefficient is given to minimize the sum of the initial construction cost and the expected cost of the seismic damage to structures[10].

5.1 Concept of optimum seismic coefficient

The factors to affect the definition of an optimum seismic coefficient from an economical viewpoint are the initial construction cost, the cost of seismic damage to the structures, the utility of repair works to local economics, the effect of port constructions on the environmental and so on. At the present time, it is very difficult to quantify these factors other than the initial construction cost and the cost of seismic damage to structures. Therefore the economical viewpoint in this report focused on these two factors for the first step to define the optimum seismic coefficient.

When the seismic coefficient becomes larger, the expected cost of seismic damage

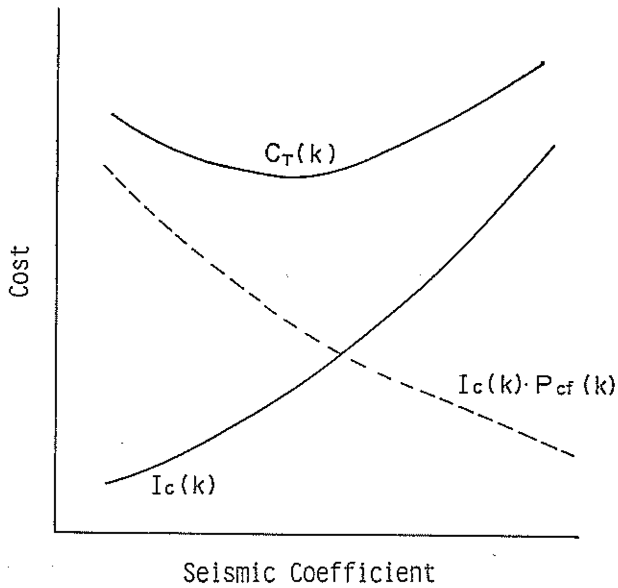

Fig. 16 Relation between cost and seismic coefficient

to structures (expected seismic cost) decreases, and the initial construction cost increases, as shown in Fig. 16. Therefore, it is believed that the sum of the initial construction cost and the expected seismic cost (Expected total cost: $C_t(k)$) shows a raised down curve with the extreme. In this report, the seismic coefficient which gives the extreme of this $C_t(k)$ is defined as an optimum seismic coefficient from an economical viewpoint.

The accuracy of estimating the expected seismic costs discussed here is not necessarily very high, considering the scattering of the expected seismic costs and that of the acceleration for the attenuation curves. However, the study on the quantitative estimation of the expected seismic cost is the first stage in earthquake engineering. It was still considered for this study to be currently useful.

5.2 Relation between initial construction cost and seismic coefficient

The initial construction cost of a given gravity revetment which was designed for the two kinds of foundation ground of a sand layer and a clay layer, and for several seismic coefficients were estimated. Figure 17 shows this initial construction cost versus seismic coefficient. The vertical axis in Fig. 17 is the ratio of the initial construction cost for each seismic coefficient to that for the ordinary condition.

The relationship between the initial construction cost and the seismic coefficient for port facilities had been reported in the study on the economical design of port facilities by Murata, Yagyu and Uchida[11]. Figure 18 shows the initial construction cost against the seismic coefficient for the gravity quaywall where the structure is of the caisson type shown in Fig. 19. It is necessary to pay attention to the price

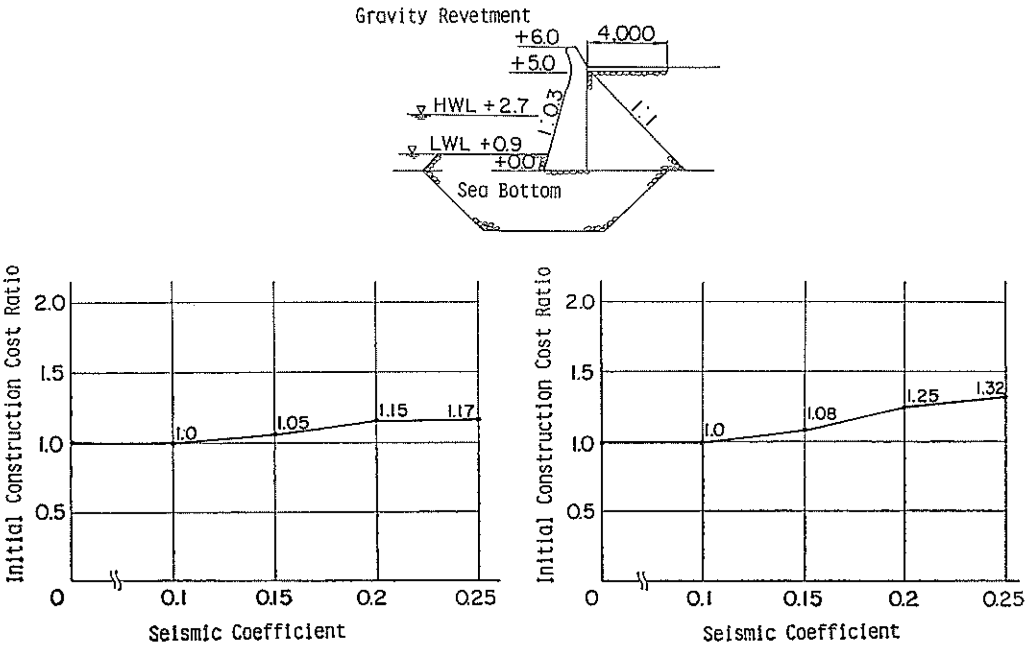

Fig. 17 Initial construction cost versus seismic coefficient (Gravity revetment)

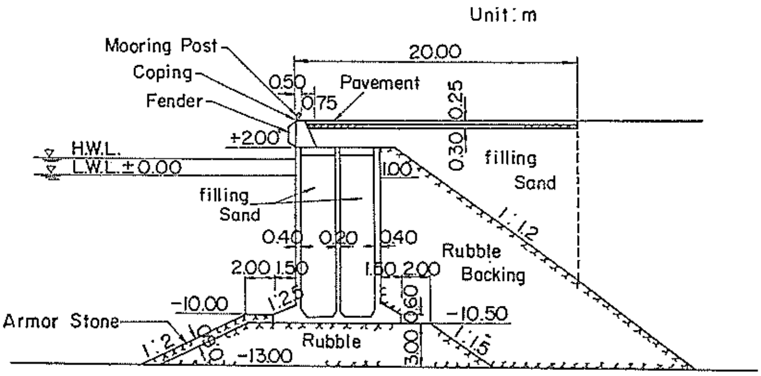

Fig. 18 Standard section of caisson type quaywall (Murata el al.)

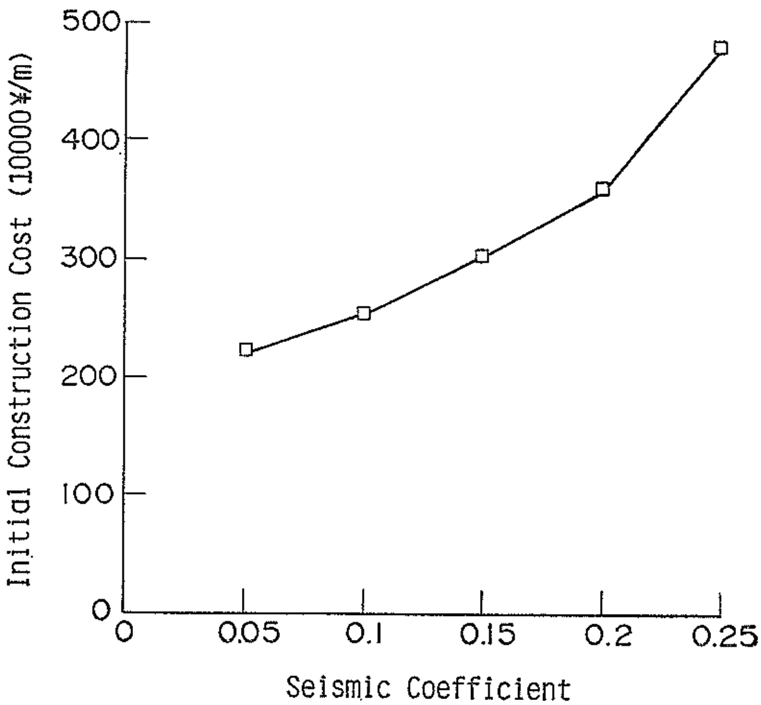

Fig. 19 Initial construction cost versus seismic coefficient (Murata el al.)

level of the year 1976 and the unit of vertical axis that is 10,000 yen/m. The increase rate of the initial construction cost for caisson type quaywall against the seismic coefficient, is larger than that for the gravity revetment in Fig. 17. The cost ratio of the construction whose seismic coefficient is between 0.25 and 0.1 is 1.3 in case of the gravity revetment, and that is about 2.0 in case of the gravity quaywall.

5.3 Expected seismic cost rate

In this paragraph, the estimation method of the expected seismic cost rate is described. The expected seismic cost rate is defined as the product of the seismic cost rate and the probability of occurrence. According to Chapter 4, the expected seismic cost rate was estimated from the ratio of the working seismic coefficient to the breaking seismic coefficient. The working seismic coefficient was obtained from the maximum ground acceleration using the relation shown in Chapter 4. Therefore, the probability of the occurrence of a seismic cost rate was defined as the probability of occurrence of the maximum ground acceleration.

(1) Cumulative distribution function and probability density function of maximum ground acceleration at Japanese ports

The probability of the occurrence of the maximum ground acceleration at a given site was studied here based on the report of Kitazawa, Uwabe and Higaki[12]. Figure 20 shows the procedure for estimating the probability of occurrence of the maximum base rock acceleration. First, the data for past earthquakes from 1885 to 1981 were collected. Next, 190 calculation points were selected along the coast in Japan. The maximum base rock acceleration at each point was then estimated from the empirical attenuation curve shown in Fig. 21. The effective distance at each point for the given earthquake was measured from the edge of the source region. On the basis of these data, the probability of occurrence of the maximum acceleration was calculated with the assumption of the Gumbel distribution. Figure 22 shows the base rock acceleration against the return period at Tokyo, Niigata and Shimonoseki. These three ports were selected from the viewpoint of probability of earthquake occurrence. According to Fig. 22, the maximum base rock accelerations

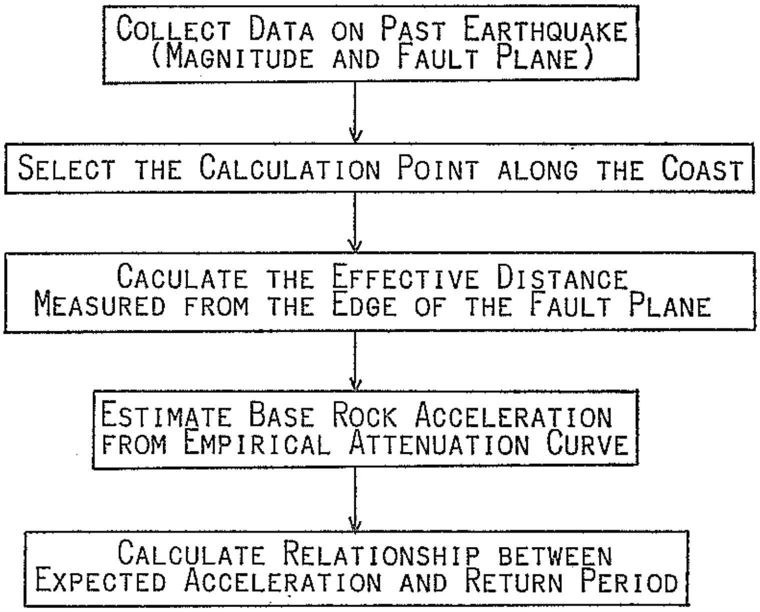

Fig. 20 Procedure to estimate probability of occurence of acceleration

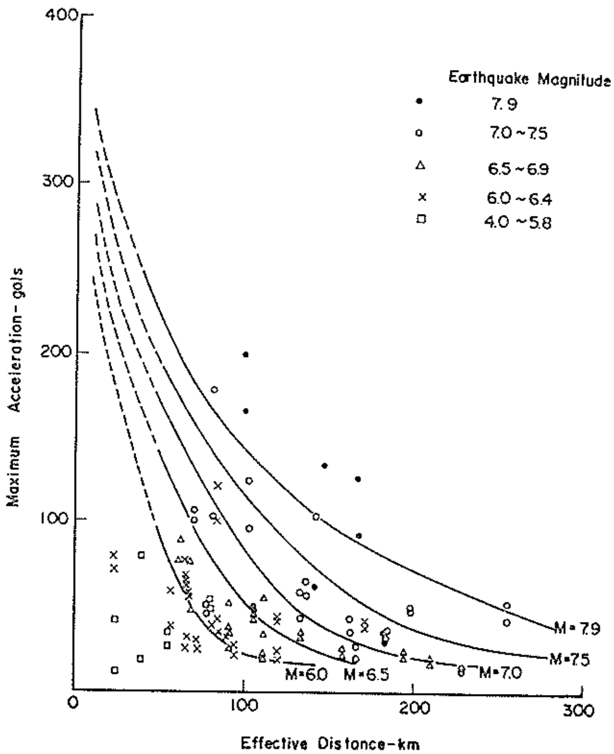

Fig. 21 Attenuation curve of maximum acceleration

for the return period of 50 years were 240 Gal at Tokyo port, 120 Gal at Niigata port and 60 Gal at Shimonoseki port.

The m-th extrimal distribution of the Gumbel distribution, the cumulative distribution function and probability density function of t durable years were obtained as follows[13),14)]:

$$f_p(X_m)=\frac{m^m}{(m-1)!}\exp\left(-m\cdot\frac{X_m-B}{A}-m\cdot e^{-\frac{X_m-B}{A}}\right) \tag{8}$$

$$\left.\begin{aligned}F_m(X_m)=&\left\{\left(1-\frac{N}{K}\right)+\frac{N}{K}\cdot\exp\left(-m\cdot e^{-\frac{X_m-B}{A}}\right)\right.\\&\left.\cdot\left(\sum_{n=1}^{m}\frac{m^{(n-1)}}{(n-1)!}\cdot e^{-(n-1)\frac{X_m-B}{A}}\right)\right\}^t\end{aligned}\right\} \tag{9}$$

$$\left.\begin{aligned}f_m(X_m)=&\frac{m^m}{(m-1)!}\cdot\frac{t\cdot N}{A\cdot K}\left\{\left(1-\frac{N}{K}\right)+\frac{N}{K}\cdot\exp\left(-m\cdot e^{-\frac{X_m-B}{A}}\right)\right.\\&\left.\cdot\left(\sum_{n=1}^{m}\frac{m^{(n-1)}}{(n-1)!}\cdot e^{-(n-1)\frac{X_m-B}{A}}\right)\right\}^{t-1}\\&\cdot\exp\left(-m\cdot\frac{X_m-B}{A}-m\cdot e^{-\frac{X_m-B}{A}}\right)\end{aligned}\right\} \tag{10}$$

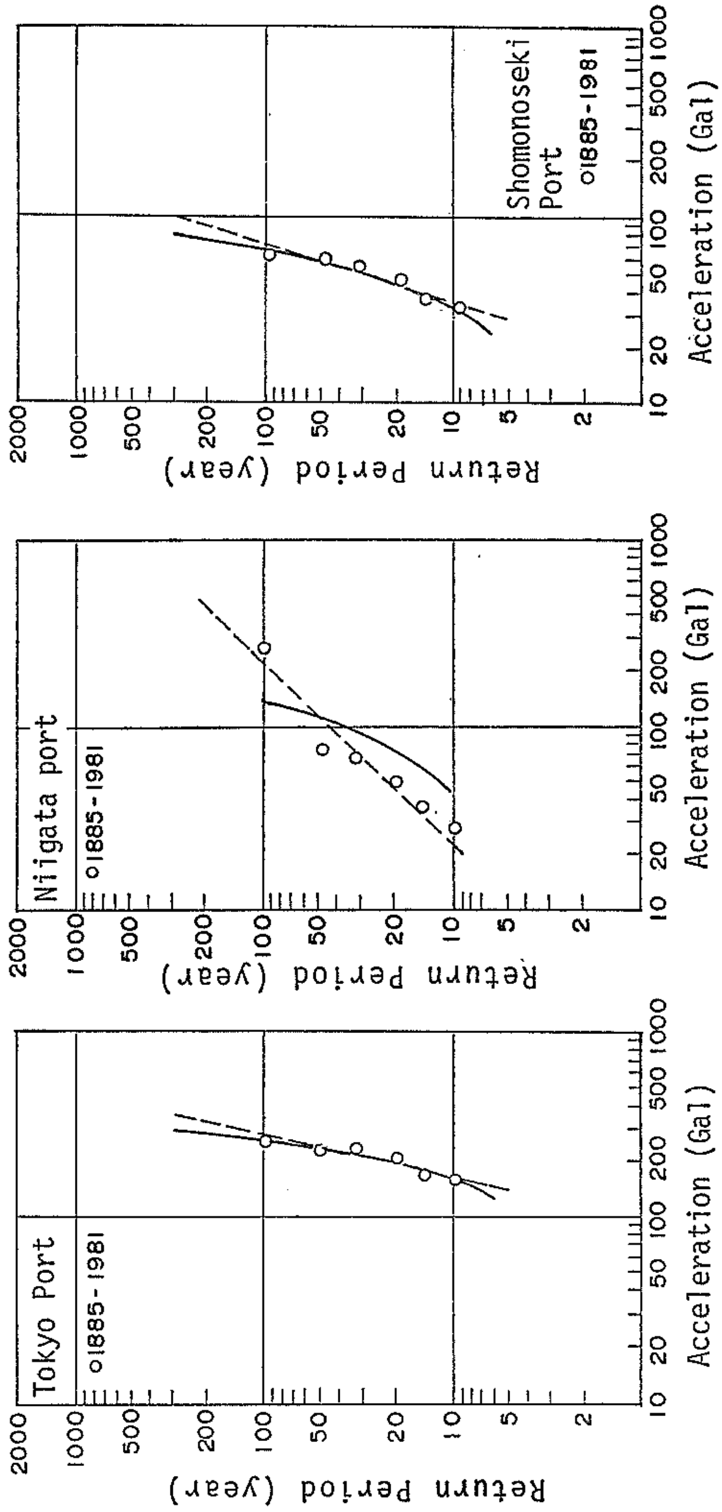

Fig. 22 Maximum base rock acceleration versus return period

where, X_m: M-th acceleration
A, B: Constant of Gumbel distribution
N: Number of data
K: Period of earthquake data
t: Durable years

Figure 23 shows the distribution function and the probability density function for Tokyo port. The probability density function of the maximum anticipated acceleration at Tokyo port for the durable years of 50 years is $f_1(x)$ in Fig. 23, and the acceleration of 240 Gal where $f_1(x)$ shows a peak the same as the expected acceleration for the return period of 50 years in Fig. 22.

(2) Expected seismic cost rate

When the distribution function of the m-th extreme is $f_m(x)$, the probability of occurrence of the m-th extreme is $f_m(x)dx$. The expected seismic cost rate

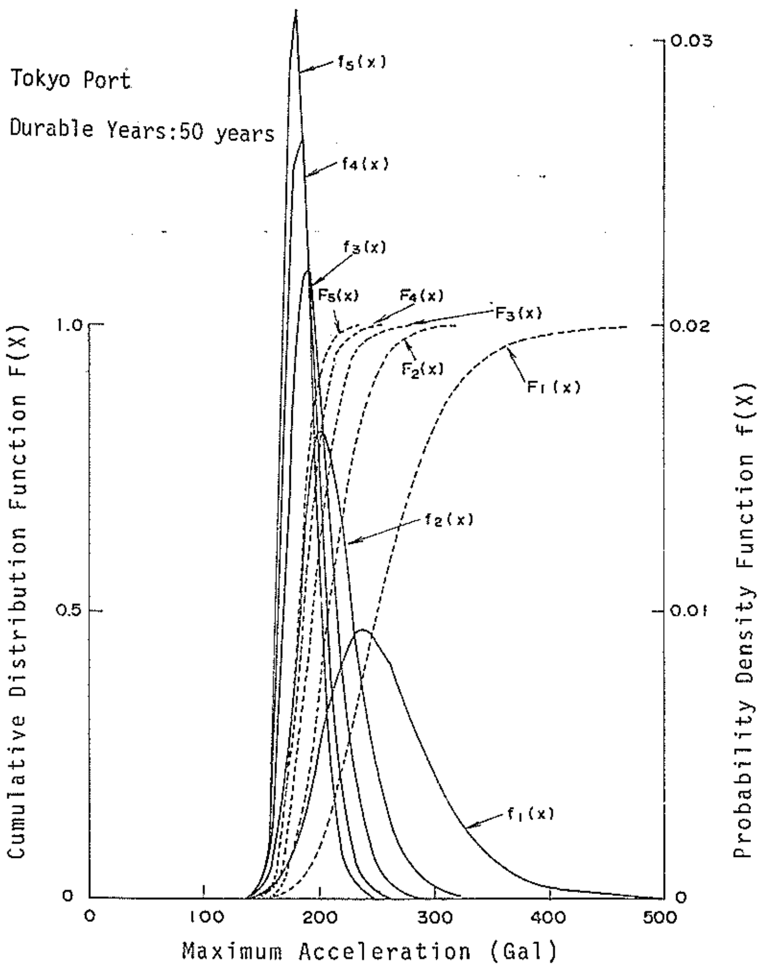

Fig. 23 Distribution function and probability density function (Tokyo port)

derived from $f_m(x)dx$ and the seismic cost rate $D(x)$ is

$$P_{cf}=\sum^{m}\int_{(X)} D(X)f_m(X)dx \tag{11}$$

Moreover, $D(x)$ is given by the equations of (6) and (7). As the extreme of large order had little influence on the expected seismic cost rate, the extremes from 1st to 5th were considered for the calculation of the expected seismic cost rate.

5.4 Optimum seismic coefficient given by expected total cost

Optimum seismic coefficients to minimize the expected total cost were calculated for Tokyo port, Niigata port and Shimonoseki port. The number of durable years was 50, and the extremes from 1st to 5th were considered. The relations between the initial construction cost and the seismic coefficient in Figs. 17 and 19 were used. As the amount of the initial construction cost in Fig. 17 was not shown, it was supposed that the initial construction cost of the ordinary condition was 1,000,000 yen/m. As the year of the price level in Fig. 19 is the year 1976, the amount of the expected seismic cost was converted in the price level of the year 1980.

The results of calculation are shown in Fig. 24 for the gravity revetment and in Fig. 25 for the gravity quaywall (Caisson type). The solid lines with symbols of × in Figs. 24 and 25 show the initial construction cost. The solid lines with

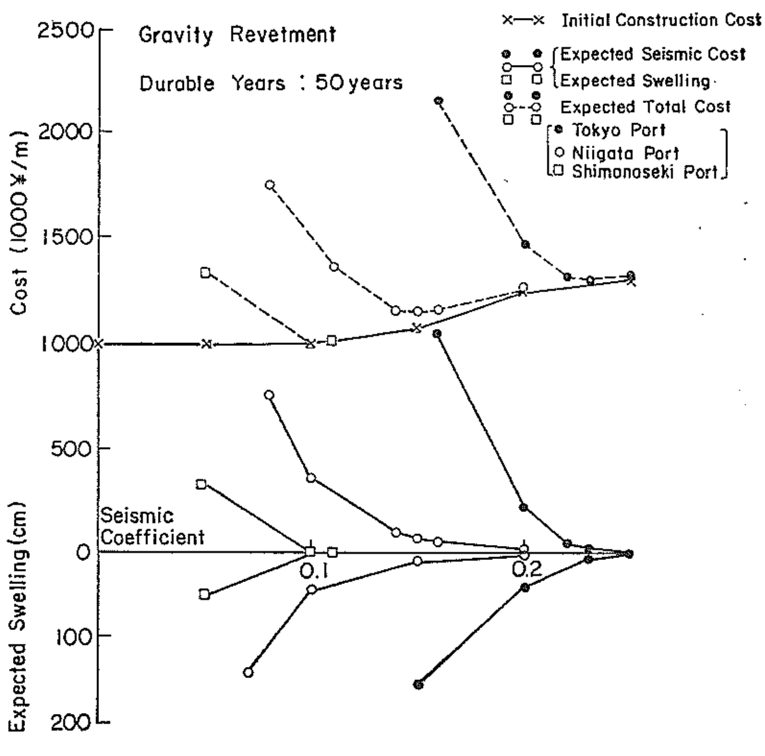

Fig. 24 Expected total cost versus seismic coefficient (Gravity revetment)

closed circles, open circles and squares show the expected seismic cost. The dotted lines show the expetced total cost. Table 5 shows the optimum seismic coefficient to minimize the expected total cost in Figs. 24 and 25.

The optimum seismic coefficients obtained here, were compared with the expected maximum ground acceleration with a return period of 50 years. Table 5 shows the seismic coefficients transformed from the expetced maximum ground accelerations

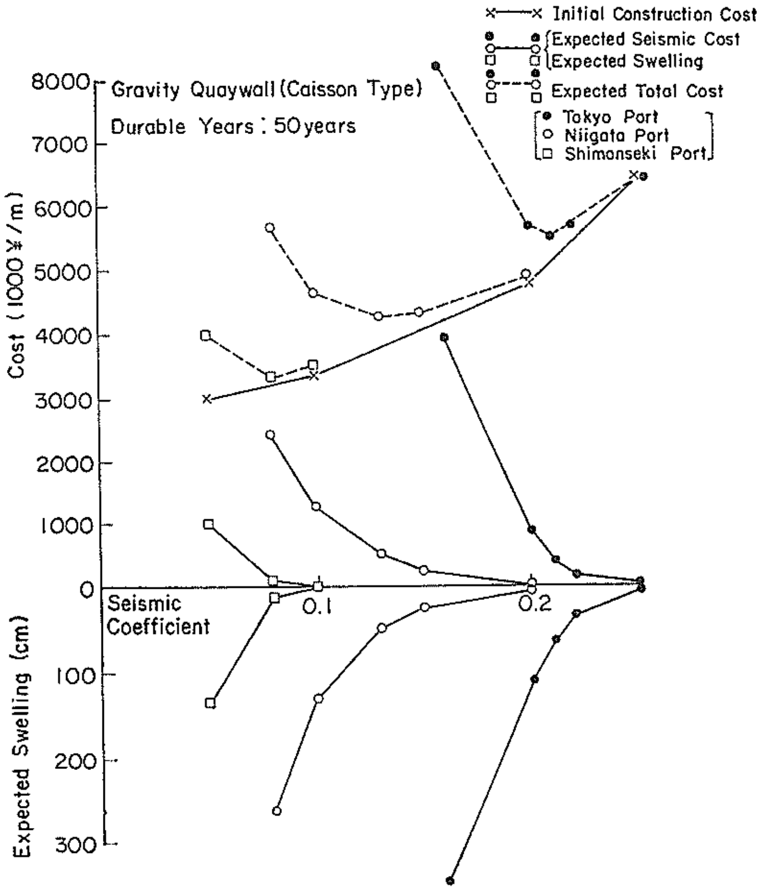

Fig. 25 Expected total cost versus seismic coefficient (Gravity quaywall)

Table 5 Optimum Seismic Coefficient

Name of port	Optimum seismic coefficient		Seismic coefficient calculated from expected acceleration for return period of 50 years
	Gravity revetment	Gravity quaywall	
Tokyo	0.23	0.21	0.21
Niigata	0.15	0.13	0.12
Shimonoseki	0.10	0.08	0.06

for a return period of 50 years in Fig. 22, using Eq. (4). In the case of gravity revetments, the optimum seismic coefficients were larger than the seismic coefficients for a return period of 50 years. In the case of gravity quaywalls, the optimum seismic coefficients were the same as the seismic coefficients at Tokyo port and were slightly larger than those at Niigata port and Shimonoseki port.

Figures 24 and 25 show the expected maximum swelling calculated from Eq. (6). The height of structures is 5 m for the gravity revetment and is 14 m for the gravity quaywall. The expected maximum swellings of the optimum seismic coefficient are as follows. In the case of a gravity revetment the expected values of maximum swelling are 5 cm at Tokyo port, 10 cm at Niigata port and 1 cm at Shimonoseki port. In the case of a gravity quaywall, the expected values of the maximum swelling are 67 cm at Tokyo port, 50 cm at Niigata port and 10 cm at Shimonoseki port. This displacement is an allowable displacement, when defined from an economical viewpoint.

6. Conclusion

Data on cases of seismic damage to gravity quaywalls were collected. Then the quantification of the earthquake damage, the classification of the failure mode and the quantitative estimation method of seismic damage to gravity quaywalls were investigated. Moreover, an optimum seismic coefficient from an economical viewpoint was studied, using the method for estimating the cost of seismic damage to gravity quaywalls. The conclusions obtained here are as follows:

1. According to the classification of the failure mode, the number of gravity quaywalls by the insufficient bearing capacity of the foundation was 33 (32% of the total) and the number of gravity quaywalls damaged by sliding was 62 (61% of the total). Therefore it was concluded that the principal cause of seismic damage to gravity quaywalls was the sliding of walls.
2. The relation between the damaged deformation ratio and the risk ratio which is the ratio of the working seismic coefficient to the breaking seismic coefficient was obtained as follows, based on the seismic damage data of gravity quaywalls in past earthquakes.

   $$R_g = -12.7 + 14.5(K_e/K_c)$$

   where, R_g: Damaged deformation ratio
   K_e: Working seismic coefficient
   K_c: Breaking seismic coefficient

   The relationship between the seismic cost rate (C_f) and the risk ratio (F_c) was derived from the regression formulae which are the equation of C_f and the damaged deformation ratio (R_g), and that of R_g and F_c.
3. The procedure to give the optimum seismic coefficient from an economical viewpoint was presented, and the optimum seismic coefficients of the gravity revetments and quaywalls were obtained from the expected total cost with the duable period of 50 years at Tokyo port, Niigata port and Shimonoseki port. The results of a comparison between these optimum seismic coefficients and the working seismic coefficient calculated from the expected maximum ground accelerations for the return period of 50 years were as follows. In the case of gravity revetments the optimum seismic coefficient was larger than the working

seismic coefficient with the return period of 50 years. In the case of gravity quaywalls the optimum seismic coefficients were same as the working seismic coefficient at Tokyo port and were slightly larger than those at Niigata port and Shimonoseki port.

(*Received on November 13, 1987*)

Acknowledgements

The author wishes to express his thanks to Dr. Yoshimi Goda, Director General of the Port and Harbour Research Institute who reviewed the manuscript and also offered useful suggestions, and also to Dr. Hajime Tsuchida, Deputy Director General of PHRI for his valuable suggestions to this study.

References

1) TSUCHIDA, H., NODA, S., INATOMI, T., UWABE, T., YAGYU, T. and MURATA, T.: Methods of Evaluation for Seismic Stability of Port and Coastal Facilities, *Technical Note of the Port and Harbour Research Institute* (*PHRI*), No. 336, June 1980.
2) UWABE, T.: Estimation of Earthquake Damage Deformation and Cost of Quaywalls based on Earthquake Damage Records, *Technical Note of PHRI*, No. 473, Dec. 1983.
3) IAI, S., KOIZUMI, K. and TSUCHIDA, H.: A New Criterion for Assessing Liquefaction Potential Using Grain Size Accumulation Curve and N-value, *Report of PHRI*, Vol. 25, No. 3, Sept. 1986, pp. 125–234.
4) KURATA, E., FUKUHARA, T. and NODA, S.: Annual Report on Strong-motion Earthquake Records in Japanese Ports (1985), *Technical Note of PHRI*, No. 547, June 1986.
5) Bureau of Ports and Harbours, The 1st District Port Construction Bureau and Port and Harbour Research Institute: Damage to Harbour Structures by the Niigata Earthquake, No. 1, Sept. 1964.
6) Bureau of Ports and Harbours, Port and Harbour Research Institute and the 1st District Port Construction Bureau: Damage to Harbour Structures by the Niigata Earthquake, No. 2, Mar. 1965.
7) MITSUHASHI, I. and NAKAYAMA, T.: Analysis of the Damage to Harbour Structures by the 1973 Nemuro-Hanto-Oki Earthquake, *Technical Note of PHRI*, No. 184, June 1974.
8) NODA, S., UWABE, T. and CHIBA, T.: Relation between Coefficient and Ground Acceleration for Gravity Quaywall, *Report of PHRI*, Vol. 14, No. 4, Dec. 1975, pp. 67–111.
9) KAWASUMI, H.: Measures of Earthquake Danger and Expectacy of Maximum Intensity throughout Japan as Infered from the Seismic Activity in Historical Times, *Bull. Earthq. Res. Inst.*, Vol. 26, 1951, pp. 469–482.
10) NONAKA, M., INOKUMA, Y. and KATAYAMA, T.: Studies on Seismic Damage Rate and Optimum Seismic Coefficient Determination of Highway Bridges, *Proc. of JSCE*, No. 340, Dec. 1983, pp. 87–96.
11) MURATA, T., YAGYU, T. and UCHIDA, T.: Some Consideration on Profitable Designing for Port and Harbour Facilities, *Proc. of 1980 Annual Research Presentations of PHRI*, Dec. 1980, pp. 233–276.
12) KITAZAWA, S., UWABE, T. and HIGAKI, N.: Expected Values of Maximum Base Rock Accelerations along Coasts of Japan, *Technical Note of PHRI*, No. 486, July 1984.
13) GUMBEL, E. J.: Statistics of Extremes (Japanese transaction version), Seisan-Gijyu-

tsu-Senta-Shinsya, June 1978.
14) UWABE, T.: Study on Quantitative Estimation of Seismic Damage to Gravity Quay-wall, *Technical Note of PHRI*, No. 548, June 1986.

List of Symbols

A : Constant of Gumbel distribution
B : Constant of Gumbel distribution
B_w : Wall width
C_f : Seismic cost rate
$D(x)$: Seismic cost rate
F_c : Risk ratio
$F_m(X_m)$: Probability density function
$f_m(X_m)$: Cumulative distribution function
$f_p(X_m)$: Gumbel's extrimal distribution
g : Acceleration of gravity
K : Period of earthquake data
K_c : Breaking seismic coefficient
K_e : Working seismic coefficient
L : Wall height
N : Number of data
P : Swelling in case that tilt angle is small
R_g : Damage deformation ratio
S_p : Measured settlement
t : Durable years
X : Swelling of face line
X_m : M-th acceleration
Y : Settlement of face line
a : Maximum ground acceleration
θ_k : Tilt angle